

# MoPE: Parameter-Efficient and Scalable Multimodal Fusion via Mixture of Prompt Experts

Jiang Ruixiang<sup>1</sup>, Lingbo Liu<sup>2</sup>, Chen Chang Wen<sup>1</sup>

<sup>1</sup>The Hong Kong Polytechnic University, HKSAR

<sup>2</sup>Peng Cheng Lab, Shen Zhen, China

rui-x.jiang@connect.polyu.hk, liulb@pcl.ac.cn, chen.changwen@polyu.edu.hk

## Abstract

Despite the demonstrated parameter efficiency of prompt-based multimodal fusion methods, their limited adaptivity and expressiveness often result in suboptimal performance compared to other tuning approaches. In this paper, we address these limitations by decomposing the vanilla prompts to adaptively capture instance-level features. Building upon this decomposition, we introduce the mixture of prompt experts (MoPE) technique to enhance the expressiveness of prompt tuning. MoPE leverages multimodal pairing priors to route the most effective prompt on a per-instance basis. Compared to vanilla prompting, our MoPE-based fusion method exhibits greater expressiveness, scaling more effectively with the training data and the overall number of trainable parameters. We also investigate regularization terms for expert routing, which lead to emergent expert specialization during training, paving the way for interpretable soft prompting. Extensive experiments across six multimodal datasets spanning four modalities demonstrate that our method achieves state-of-the-art results for prompt fusion, matching or even surpassing the performance of fine-tuning while requiring only 0.8% of the trainable parameters.

## Introduction

Unimodal pre-trained models like BERT (Radford et al. 2019) and Swin Transformer (Liu et al. 2021b) have excelled in transferring capabilities to a wide range of tasks. By comparison, extending the pretraining-finetuning paradigm to multimodal applications involves additional complexities, particularly regarding flexibility and cost. First, the modality-paired pretraining can be inflexible due to its dependence on specific configurations. This can limit flexibility when there is a scarcity of certain modality pairs, or when new architectures emerge, necessitating resource-intensive retraining. In contrast, unimodal pretrained models are more readily available and offer greater flexibility, as they can be independently updated and combined for multimodal tasks. Second, as these foundation models scale in size, fine-tuning them becomes increasingly expensive, which further restricts their application to downstream tasks. To democratize foundation models, a compelling question arises: *How can we efficiently combine separately pretrained unimodal models for multimodal tasks?*

Copyright © 2025, Association for the Advancement of Artificial Intelligence (www.aaai.org). All rights reserved.

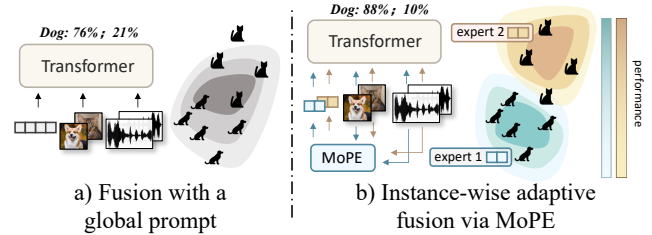


Figure 1: **High-level motivation of MoPE-based multimodal fusion.** (a) Vanilla prompt tuning learns a globally shared long prompt for all instances, which may not be optimal for each instance. (b) MoPE decomposes the global prompt into multiple short and specialized prompt experts to improve its adaptivity and expressiveness.

While originally proposed for transfer learning (Li and Liang 2021; Jia et al. 2022; Zhou et al. 2022b), recent research has revealed that prompt tuning could also be a parameter-efficient paradigm for multimodal fusion (*i.e.*, prompt fusion). Typically, this is achieved by representing one modality with several prompts, which are fed into the frozen Transformer of another modality to achieve fusion (Tsimpoukelli et al. 2021; Liang, Zhao, and Schütze 2022; Li et al. 2023; Yang et al. 2022b). However, directly using prompts for fusion could yield suboptimal results, particularly due to their limited adaptivity and scalability. Notably, while prompt tuning generally performs well in low-data regimes, it can be less effective when applied to full-shot training on the entire dataset with a challenging objective (Gao et al. 2022; Liang, Zhao, and Schütze 2022; Tsimpoukelli et al. 2021; Yang et al. 2022a; Lester, Al-Rfou, and Constant 2021). This reduced efficacy could be attributed to at least two factors. First, the vanilla prompt was originally developed for unimodal learning, which optimizes globally-shared prompts for all instances (Jia et al. 2022; Li and Liang 2021; Tsimpoukelli et al. 2021). When directly applied for prompt fusion (Tsimpoukelli et al. 2021; Li et al. 2023; Liang, Zhao, and Schütze 2022), it fails to adaptively exploit the multimodal interplay and can lead to sub-optimal representations for each input instance. Second, the relatively limited representation power (compared to fine-tuning) can lead to underfitting in multimodal datasets with a long-tail

distribution and complex cross-modal mapping (Liu et al. 2021a; Petrov, Torr, and Bibi 2023; Wang et al. 2023).

To address these challenges, increasing the number of learnable prompts, known as “*length-scaling*”, appears to be a straightforward solution. However, numerous studies have shown that the performance gains from length-scaling quickly reach saturation in both transfer-learning (Gao et al. 2022; Lester, Al-Rfou, and Constant 2021) and fusion settings (Liang, Zhao, and Schütze 2022; Tsimpoukelli et al. 2021; Yang et al. 2022a). Furthermore, over-length prompts may even lead to worse results (Jia et al. 2022; Yang et al. 2022a; Khattak et al. 2023; Li and Liang 2021; Kim et al. 2023). Recent theoretical analyses have substantiated these empirical observations, highlighting the limited expressiveness of prompt tuning (Wang et al. 2023; Petrov, Torr, and Bibi 2023). Overall, evidence from both empirical and theoretical analyses reveals that simply increasing prompt length is insufficient to address the limitations of prompt fusion.

To improve the adaptivity and expressiveness of prompt fusion, we propose decomposing the unified, long prompt into multiple short prompts with specialized responsibilities, as depicted in Fig. 1. We introduce an instance-wise adaptive prompt decomposition that separates the vanilla prompt into static, dynamic, and mapped prompts to adaptively capture global and local features. The foundation of our dynamic prompt generation lies in the proposed MoPE (Mixture of Prompt Experts) design, where we maintain a fixed prompt length in the self-attention and enhance expressiveness by learning multiple prompt experts and a multimodal router to select the most suitable prompt for each instance.

We systematically compare our MoPE-based fusion with previous prompt fusion methods on a total of six datasets, and demonstrate consistently superior performance with higher parameter-efficiency. Furthermore, we showcase the superior scalability of our method both in terms of parameter and data. Our analysis indicates that increasing the number of experts (i.e., “*expert-scaling*”) is more scalable than length-scaling, with monotonic performance gains and the avoidance of performance deterioration with an overly-long prompt. Our method also scales better with more training data. By introducing regularization terms for expert routing, we observe the emergence of specialized prompt experts after end-to-end training, resulting in high interpretability. Our key contributions are summarized as follows:

- We propose an instance-wise adaptive prompt decomposition, which decomposes the vanilla prompt into static, dynamic and mapped prompt.
- We introduce the MoPE technique for instance-wise dynamic prompt generation, which scales up the expressiveness of prompt tuning for multimodal fusion.
- A combination of regularization terms is studied to aid specialization of prompt experts.
- Extensive experiments on six datasets spanning four modalities demonstrate state-of-the-art performance and parameter efficiency for prompt-based multimodal fusion.

## Related Works

**Prompt Tuning for Transfer Learning.** Prompt tuning (Li and Liang 2021; Lester, Al-Rfou, and Constant 2021) learns continuous token embeddings as additional input to a frozen pretrained model for transfer learning of Transformer-based models. It is widely used in various modalities (Jia et al. 2022; Bahng et al. 2022; Liu et al. 2022; Lin et al. 2023; Jiang, Liu, and Chen 2023; Khattak et al. 2023; Zhou et al. 2022a). A common observation is good transfer learning performance in low-shot scenarios, yet its performance is less comparable to fine-tuning when abundant training instances are available (Li and Liang 2021; Gao et al. 2022). Moreover, increasing prompt length quickly reaches performance saturation, and over-length prompts might lead to worse results (Yang et al. 2022a; Jia et al. 2022; Kim et al. 2023). Recent theoretical analyses (Petrov, Torr, and Bibi 2023; Wang et al. 2023) reveal that the expressiveness of prompt tuning is lower than that of fine-tuning. In this work, we tackle this challenge by scaling up the expressiveness of prompts with a Mixture of Experts (MoE)-like design.

**Multimodal Fusion via Prompt.** Apart from model adaptation, prompts can also be used to fuse separately pretrained *unimodal models* for multimodal tasks. Frozen (Tsimpoukelli et al. 2021) first introduced a method where the visual representation is mapped as a few input tokens to query frozen language models (LMs). PromptFuse and BlindPrompt (Liang, Zhao, and Schütze 2022) improved upon this by introducing tunable prompts to the LM for cross-modal alignment. PICa (Yang et al. 2022b) translates images into discrete text captions to prompt frozen LMs. These methods treat tokens from different modalities independently and lack cross-modal interaction. Recently, PMF (Li et al. 2023) introduced an interactive prompt fusion method for the vision and text modalities, building on the strong assumption that both encoders are white-box and have the same Transformer architecture. In this paper, we investigate how to adaptively interact with two or more modalities with minimal assumptions about the model architecture.

**MoE in Transformers.** MoE is a computationally efficient technique to scale up models, including Transformers (Lepikhin et al. 2020; Riquelme et al. 2021; Mustafa et al. 2022; Fedus, Zoph, and Shazeer 2022). The fundamental approach involves inserting MoE layers, usually composed of multiple feed-forward networks (FFNs) acting as experts, into the standard Transformer architecture. A router is learned to route each token embedding to the most suitable expert(s) for reducing computational overhead (Qin and Eisner 2021; Riquelme et al. 2021; Shazeer et al. 2017). In this paper, we do not focus on reducing computational cost; instead, we introduce the MoE design into prompt fusion to scale up its adaptiveness and expressiveness.

## Method

### Preliminary: Vanilla Prompt Tuning

Consider a Transformer (Vaswani et al. 2017) or its variants used to extract features from an embedded input sequence  $\mathbf{x}^0 \in \mathbb{R}_{s \times d_x}$ , where  $s$  is the sequence length and  $d_x$  is the

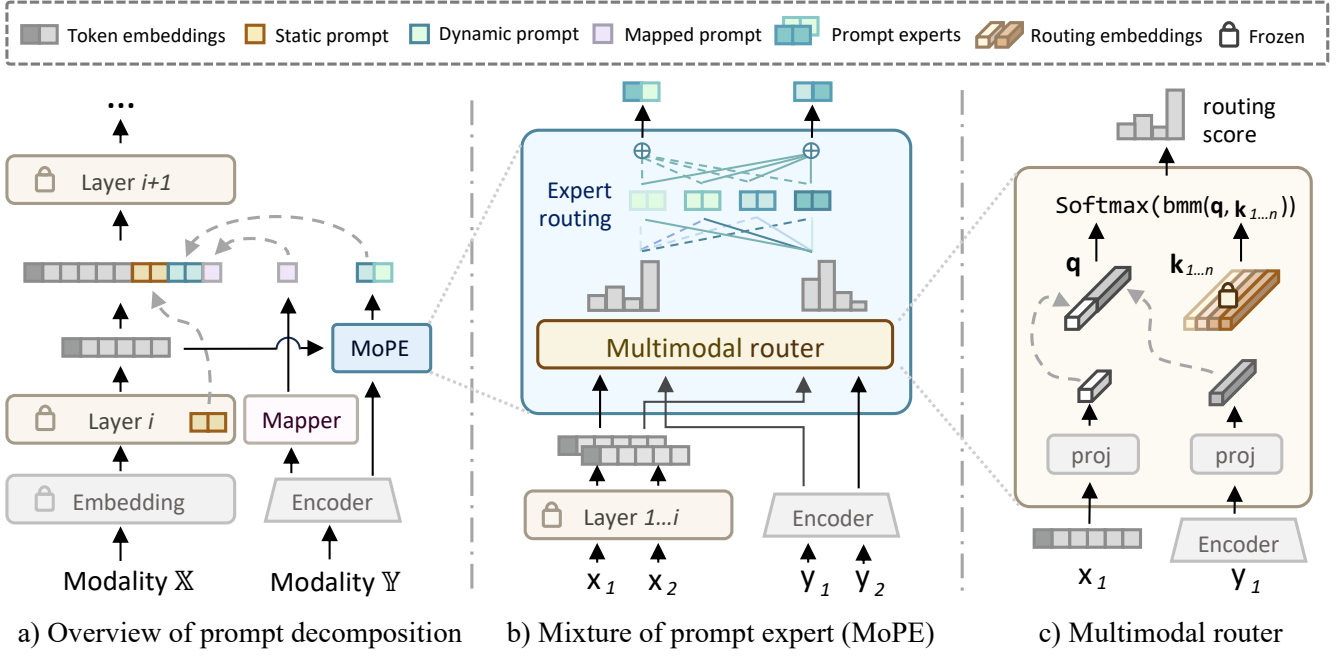


Figure 2: **Architecture overview.** a) A sequential fusion pipeline is used, using modality  $\mathbb{Y}$  to guide the prompting of modality  $\mathbb{X}$  through our prompt decomposition. (b) We introduce MoPE, which utilize the multimodal pairing as a prior to route the most suitable dynamic prompt for each instance; (c) Inside the multimodal router, we project the representation from each modalities. The concatenated embedding is used to match the routing embedding paired with each experts for routing score calculation. Better viewed with color.

embedding dimension. Prompt-tuning freezes all pre-trained parameters and optimize a small amount of continuous embeddings (*i.e.*, prompts)  $\mathbf{P} \in \mathbb{R}_{l \times d}$  concatenated to the input of each layer, where  $l$  is length of the prompt. The input of the  $i$ -th layer  $L^i$  could be denoted as:

$$\hat{\mathbf{x}}^i = [x_0^{i-1}, \mathbf{P}, \mathbf{T}^{i-1}] \quad (1)$$

where  $x_0^{i-1} \in \mathbb{R}_{d_x}$  denotes the [CLS] token,  $\mathbf{T}^{i-1} \in \mathbb{R}_{s \times d_x}$  is the token embedding from the previous layer, and  $[\cdot, \cdot]$  denotes the concatenation operation.

Succinctly, prompt tuning works by biasing the pretrained attention pattern in each Transformer layers (Petrov, Torr, and Bibi 2023). As opposed to fine-tuning, this biasing has strictly limited expressiveness in theory (Petrov, Torr, and Bibi 2023; Wang et al. 2023), meaning that there are tasks that are un-learnable even with  $l \rightarrow \infty$ . The empirical expressiveness of vanilla prompting is even lower than its theoretical upper bound, due to competing optimization when  $l > 1$  (Petrov, Torr, and Bibi 2023). In other words, although longer prompt gives more trainable parameters, finding such a long prompt becomes challenging, and a suboptimal long prompt can lead to performance degradation instead. In this paper, we do not aim to increase the theoretical upper bound of prompt-tuning; instead, we approach the problem by narrowing the gap between its empirical and theoretical expressiveness.

## Instance-wise Adaptive Prompt Decomposition

Previous prompt fusion methods (Liang, Zhao, and Schütze 2022; Yang et al. 2022b) optimize a global prompt that is shared across all instances, neglecting the interplay between different modalities and instance-specific features. With paired multimodal input as a prior, we aim to instance-wisely condition the prompting of one modality on the other(s) for better adaptivity. To achieve this goal, we first adopt a sequential fusion pipeline. Let  $x \in \mathbb{X}, y \in \mathbb{Y}$  be a pair of multimodal inputs, and  $\mathcal{E}_X, \mathcal{E}_Y$  be the encoder of each modality. Depending on the task intrinsic, we assign a fusion direction where the encoding of main modality  $\mathbb{X}$  is conditioned on representation of complementary modality(ies)  $\mathbb{Y}$ .

Building upon the sequential pipeline, we decompose the vanilla prompt vector  $\mathbf{P}$  used in  $\mathcal{E}_X$  into three types of specialized prompts  $[\mathbf{P}_s, \mathbf{P}_d, P_m]$ . The static prompt  $\mathbf{P}_s \in \mathbb{R}_{l \times d_x}$  is a globally-shared prompt vector that is shared for all instances. The dynamic prompt  $\mathbf{P}_d \in \mathbb{R}_{l \times d_x}$  are adaptive to different instances. To synthesize it, we first encode global-level feature from the complementary modality  $\psi_y = \mathcal{E}_Y(y) \in \mathbb{R}_{d_y}$ , and utilize a MoPE module  $R(\cdot, \cdot)$  to generate the dynamic prompt. Additionally, we apply a lightweight mapper  $f_m(\cdot)$  to map the complementary feature into a single prompt  $P_m \in \mathbb{R}_{d_x}$ , which injects fine-grained cross-modal information. In summary, the input of layer  $L^i$  of  $\mathcal{E}_X$  becomes:

$$\hat{\mathbf{x}}^i = [x_0^{i-1}, \underbrace{\mathbf{P}_s, R(x_0^{i-1}, \psi_y), f_m(\psi_y)}_{\text{Decomposed prompts}}, \mathbf{T}^{i-1}] \quad (2)$$

The whole process is illustrated in Fig. 2-(a).

### Mixture of Prompt Experts

To mitigate the negative impact on optimizing a long prompt and to improve the adaptiveness of dynamic prompt, we propose to learn multiple short prompts with a MoE-like design. To be more specific, we use MoPE module in each prompt-tuned Transformer layers  $L^i$  to generate the dynamic prompt in a scalable way. A MoPE module consists of a router,  $k$  prompt experts and their associated *routing embeddings*  $\{(\mathbf{E}_j, \mathbf{k}_j)\}_{j=1}^k$  where  $\mathbf{E}_i \in \mathbb{R}_{l \times d}$  is an expert,  $\mathbf{k}_i \in \mathbb{R}_{d_r}$  is its routing embedding, and  $d_r$  is the dimension of routing embedding.

We route each instance based on representations of all modalities, as illustrated in Fig. 2-(b,c). The router is parameterized as two layer-specific linear transformations  $\mathbf{W}_y^i \in \mathbb{R}_{d_y \times d_c}$  and  $\mathbf{W}_x^i \in \mathbb{R}_{d_x \times d_i}$ , where  $d_c, d_i$  are the dimension of cross-modal and inter-modal routing embedding, respectively, and  $d_i + d_c = d_r$ . The cross-model embedding is projected from  $\psi_y$ , while inter-model embedding is calculated over the global-level feature (typically represented as the [CLS] token) from previous layer  $L^{i-1}$ . Finally, we concatenate both embeddings to get an multimodal query embedding  $\mathbf{q} \in \mathbb{R}_{d_r}$ , and compute the dot product with the routing embeddings of all available experts. The routing score  $\mathbf{r}$  is calculated by:

$$\mathbf{q} = [\psi_y \mathbf{W}_y^i, x_0^{i-1} \mathbf{W}_x^i], \quad \mathbf{r}_j = \frac{\exp(\mathbf{q}^\top \mathbf{k}_j / \tau + \epsilon)}{\sum_{n=1}^k \exp(\mathbf{q}^\top \mathbf{k}_n / \tau + \epsilon)} \quad (3)$$

where  $\tau = 0.1$  is the temperature hyper-parameter, and  $\epsilon$  is sampled noise (Riquelme et al. 2021). When there are more than one complementary modality, the additional embedding could be easily extended by learning additional projections. The dynamic prompt is obtained by a convex combination of all experts at this layer according to the routing score:

$$\mathbf{P}_d = \sum_{j=1}^k \mathbf{r}_j \mathbf{E}_j \quad (4)$$

### Regularizing Expert Routing

We empirically find that a few experts tend to dominate across all instances during training, a phenomenon that has also been observed in previous MoE methods (Eigen, Ranzato, and Sutskever 2013; Shazeer et al. 2017). In this section, we introduce methods to circumvent degenerated routing and aid expert specialization.

**Orthogonal Routing Embedding.** To avoid the expert being selected in initialization being exposed to a larger gradient signal, we freeze the routing embeddings  $\{\mathbf{k}_j\}_{j=1}^k$  to suppress self-reinforcing expert domination. Our finding indicate that an orthogonal initialized (Saxe, McClelland, and

Ganguli 2013) and non-learnable routing embedding outperform learned one, while requiring fewer trainable parameters.

**Importance Loss.** To further aid expert specialization, we add an additional importance loss (Shazeer et al. 2017; Riquelme et al. 2021) to penalize dominant experts. For a batch of input  $\mathbf{B} = \{(x_0, y_0), (x_1, y_1), \dots, (x_b, y_b)\}$ , the importance of expert- $j$  is defined as the summed routing score in this batch,  $\text{Imp}(\mathbf{E}_j) = \sum_{(x,y) \in \mathbf{B}} \mathbf{r}_j$ . The importance loss is calculated as the mean coefficient of variation of all experts’ importance averaged across all layers:

$$\mathcal{L}_{imp} = \sum_{\text{All layers}} \sigma \left( \left( \frac{\text{std}(\{\text{Imp}(\mathbf{E}_j)\}_j^k)}{\text{mean}(\{\text{Imp}(\mathbf{E}_j)\}_j^k)} \right)^2 ; \gamma \right) \quad (5)$$

where  $\sigma(\cdot)$  is the stop-gradient operator to prevent error propagation of this loss term when the coefficient of variation is less than a pre-defined threshold  $\gamma = 0.1$ . While this loss was initially proposed for balancing computational budgets (Shazeer et al. 2017; Riquelme et al. 2021), we adapt its use for promoting expert specialization. We add an additional threshold constraint due to our instance-wise routing, which is more likely to have a larger coefficient of variation than per-token routing.

## Experiments

**Datasets.** Following previous prompt fusion methods (Liang, Zhao, and Schütze 2022; Li et al. 2023), we conduct experiments on **MM-IMDB** (Arevalo et al. 2017) and **UPMC Food-101** (Wang et al. 2015) for classification, **SNLI-VE** (Xie et al. 2019) for visual entailment (with image premise only), **MUSTARD** (Castro et al. 2019) for sarcasm detection in speaker-dependent setting. We additionally test our method on the **RefCOCO** and **RefCOCO+** (Kazemzadeh et al. 2014) dataset for referring expression segmentation.

**Architecture Details.** In main experiment, we use Swin-B (Liu et al. 2021b) as the image encoder, Bert-base (Devlin et al. 2018) as the text encoder, Wav2Vec2 (Baevski et al. 2020) as the audio encoder. For the video modality, we use the same frame averaging technique by adapting a ViT (Dosovitskiy et al. 2020) encoder, which follows PromptFuse (Liang, Zhao, and Schütze 2022). Image is used as main modality unless otherwise specified. Following the experiment setup in (Jia et al. 2022; Li et al. 2023; Liang, Zhao, and Schütze 2022), we finetune dataset-specific heads. We implement the mapper as a two-layer MLP with GeLU nonlinearity. Regarding prompt, we set  $l = 6$  and use  $k = 16$  experts by default, and the prompts are applied to all layers of the main modality encoder. Vanilla prompt tuning (Li and Liang 2021) with  $l' = 4$  is used to tune the  $\mathcal{E}_Y$ .

**Training Details.** All models are trained for 20 epoches, using the AdamW (Loshchilov and Hutter 2017) optimizer with a learning rate of  $4 \times 10^{-4}$  for main modality and  $5 \times 10^{-4}$  for complementary modality. All models are trained with a RTX-4090 GPU.

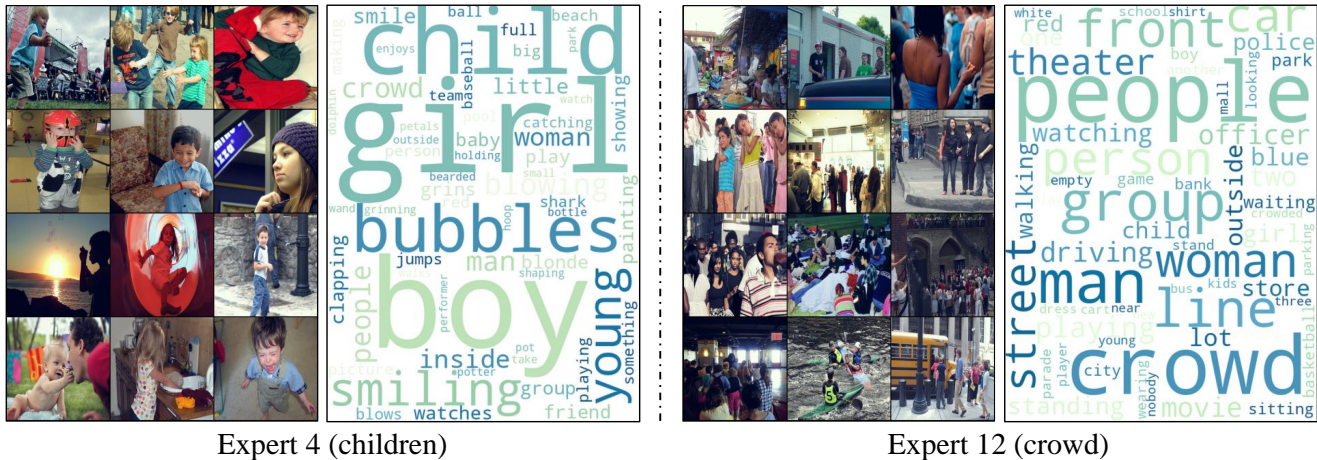


Figure 3: **Interpretable prompting through MoPE routing.** Different experts in MoPE learn to specialize in specific types concepts. In this example, expert-4 is specialized for children while expert-12 focuses on crowds.

Further experiment details could be found in the Supplementary Material.

**Compared Methods.** We consider following baselines:

*ImgOnly / TextOnly.* Fine-tune one encoder only, and the input of the other modality is discarded.

*P-ImgOnly / P-TextOnly.* Only prompt-tune one encoder.

*LateConcat.* This baseline involves fine-tuning both encoders, concatenating their features, and learn a linear head for classification.

*P-LateConcat.* Similar as *LateConcat* but prompt-tune each encoder instead of fine-tuning.

*SeqFuse.* This baseline first extracts features from the complementary modality and maps them to the embedding space of the main modality encoder by a MLP. Both encoders are fine-tuned. This is a strong baseline that can be considered as our method without MoPE, but with all parameters fine-tuned.

*P-SeqFuse.* Prompt-tune each encoders in *SeqFuse*.

In addition to these baselines, we also compare our methods with existing prompt-based fusion methods, including MMBT (Kiela et al. 2019), Frozen (Tsimpoukelli et al. 2021), PromptFuse and BlindPrompt (Liang, Zhao, and Schütze 2022), and PMF (Li et al. 2023). Among these methods, the setting in PromptFuse (Liang, Zhao, and Schütze 2022) is the most similar to ours, as it also assumes one modality to be a black-box and is by design compatible with more than two modalities. To ensure a fair comparison, all prompt-tuning baselines utilize the same prompt length ( $l = 6$ ) as our method.

**Quantitative Comparison with Previous Methods**

**Multimodal Classification.** The quantitative results on multimodal classification on all methods are summarized in Tab 1. The metric on SNLI-VE, UPMC Food-101 is accuracy (%), MM-IMDB is F1-Macro and F1-Micro (%), and on MuSTARD is precision (%). We also list the inference time (in milliseconds) and number of trainable parameters (in million) for each method.

Our method outperforms all prompt-based methods, and is competitive with fine-tuning. Specifically, when compared with the fine-tuning baselines, *SeqFuse* and *LateConcat*, our method delivers competitive accuracy on the UPMC Food-101 dataset and superior results on the SNLI-VE, MM-IMDB and MuSTARD datasets, while requiring as few as 0.8% of the trainable parameters.

The proposed method also outperforms all existing prompt fusion methods, including PromptFuse (Liang, Zhao, and Schütze 2022), BlindPrompt (Liang, Zhao, and Schütze 2022), and PMF (Li et al. 2023). Notably, our method ( $k = 4$ ) outperforms the current SOTA, PMF, by a significant margin on all datasets, while requiring 37% fewer parameters. Moreover, our method has a weak assumption than PMF, which assumes both encoders share the same Transformer architecture, making it hard to be extended to other modalities and other model architectures.

**Referring Expression Segmentation.** Previous prompt fusion methods mainly test their performance on classification (Li et al. 2023; Liang, Zhao, and Schütze 2022; Tsimpoukelli et al. 2021). The improved expressiveness of MoPE allows learning of harder tasks, for example, referring image segmentation. Following experiment setting in VPT, We additionally finetune a SeTR-PUP (Zheng et al. 2021) head for segmentation. The result is summarized in Tab. 2. Our proposed method achieves the best result among all compared methods. In particular we outperform the fine-tuning baseline *SeqFuse*, which suffers from catastrophic forgetting problem on this task.

**Qualitative Result of MoPE Routing**

Through training, prompt experts in MoPE spontaneously specialize, and we present two examples in Fig. 3. We visualize the expert with the highest score as the routed expert for each instance pair. In the provided examples, we observe that expert-4 specialize in children-related concepts, while expert-12 focuses on crowds. These examples also demonstrate the interpretability of MoPE, as opposed to black-box

	Method	Param	Speed (ms)	I+L			A+L	A+V+L
				<u>SNLI-VE</u> Acc (↑)	<u>UPMC Food</u> Acc (↑)	<u>MM-IMDB</u> F1-macro/F1-micro (↑)	<u>MUsTARD</u> Pre (↑)	<u>MUsTARD</u> Pre (↑)
<i>fine-tuning</i>	ImgOnly	86.9M	16.45±0.2	33.34	75.64	39.21/53.85	-	-
	TextOnly	109.0M	7.28±0.9	69.58	86.92	58.80/65.37	65.41	65.41
	LateConcat	196.0M	22.79±0.9	72.01	93.19	60.43/67.77	68.82	69.40
	SeqFuse	197.0M	23.32±1.2	74.28	93.73	59.22/66.34	68.13	71.35
	MMBT	196.5M	15.91±1.2	67.58	94.10	60.80/66.10	-	-
<i>prompt-tuning</i>	P-ImgOnly	0.1M	21.01±1.1	33.34	76.65	33.70/50.04	-	-
	P-TextOnly	0.1M	7.57±1.2	64.86	81.01	52.19/61.16	59.27	59.27
	P-LateConcat	1.3M	28.59±2.1	64.29	90.27	56.95/64.23	60.71	65.17
	P-SeqFuse	1.1M	28.52±1.9	65.01	81.27	55.57/63.98	63.72	65.73
	P-MMBT	0.9M	16.71±1.3	67.58	81.07	52.95/59.30	-	-
	PromptFuse	<0.1M	28.75±0.9	64.53	82.21	48.59/54.49	63.76	64.20
	BlindPrompt	<0.1M	29.52±1.2	65.54	84.56	50.18/56.46	62.01	63.80
	PromptFuse(†)	0.1M	29.26±1.7	64.94	82.14	50.78/60.96	64.73	66.29
	PMF	2.5M	32.21±0.8	71.92	91.51	58.77/64.51	-	-
	Ours ( $k=4$ )	1.6M	30.47±1.4	73.14	91.54	61.93/68.19	67.12	67.35
	Ours ( $k=16$ )	2.6M	30.44±1.3	<b>73.59</b>	<b>92.05</b>	<b>62.01/68.24</b>	<b>68.73</b>	<b>69.94</b>

Table 1: **Quantitative results on multimodal classification.** Our method achieve the best performance and parameter-efficiency against all prompt-fusion methods. I: Image, L: Language, A: Audio, V: Video. The main modality is underlined, and the best prompt tuning method is **bold**, and (†): Our re-implementation with prompt applied to all layers.

Method	Param	RefCOCO, mIOU(↑)			RefCOCO+, mIOU(↑)		
		val	testA	testB	val	testA	testB
SeqFuse	231.0M	53.48	55.76	52.03	40.22	42.2	37.91
P-SeqFuse	35.1M	47.69	46.23	45.81	30.66	31.48	28.79
PromptFuse(†)	35.1M	43.23	39.71	47.74	27.72	33.37	23.67
Ours	35.5M	<b>58.40</b>	<b>60.03</b>	<b>53.23</b>	<b>43.80</b>	<b>46.12</b>	<b>38.88</b>

Table 2: **Quantitative result on referring image segmentation** We report the total number of parameters in million (including the trainable segmentation head), and metrics (mIOU) on RefCOCO and RefCOCO+.

conditional prompt such as CoOp (Zhou et al. 2022b). More visualizations could be found in supplementary material.

## Analysis and Discussion

In this section, we systematically analyze the effects of our proposed design through ablation studies. We show that our MoPE-based fusion method is more adaptive and scalable for multimodal fusion compared to existing approaches.

**Our decomposed prompts are collaborative.** We ablate each type of prompt in our instance-wise prompt decomposition, with results across 3 random seeds reported in Tab. 3. Our full method achieves the best performance, indicating effective prompt collaboration. Adding the dynamic prompt yields gains of 13.5%, 13.26%, 8.4%/6.5% on all datasets, this is different from previous methods (Liang, Zhao, and Schütze 2022; Tsimpokelli et al. 2021) where modalities don’t explicitly interact. Without the mapped prompt, fine-grained information from complementary modalities is lost, causing significant drops. The static prompt is also necessary, acting as a special expert always routed for capturing global-level features.

Prompt	SNLI-VE(↑)	UPMC Food(↑)	MM-IMDB(↑)
$[P_s]$	33.34±.01	76.65±.07	33.70±.55/50.04±.27
$[P_d]$	64.26±.41	74.79±.38	46.54±.77/59.71±.35
$[P_m]$	33.47±.32	73.06±.12	24.84±.14/45.10±.32
$[P_s, P_d]$	66.76±.26	75.13±.14	49.09±.43/60.89±.37
$[P_s, P_m]$	65.01±.18	81.27±.22	55.57±.63/63.98±.35
$[P_d, P_m]$	71.39±.59	91.21±.16	60.15±.37/67.14±.17
$[P_s, P_d, P_m]$	<b>73.59±.15</b>	<b>92.05±.11</b>	<b>62.01±.21/68.24±.12</b>

Table 3: **Ablation on prompt decomposition.** The results from all combinations of mapped prompt, dynamic prompt, and static prompt are presented. Our full method with all prompts achieves the best result.

### Expert-scaling is more expressive than length-scaling.

To study the expressiveness of MoPE, we compare expert-scaling with length-scaling. Our starting point for MoPE is  $l = 6$  prompts and  $k = 2$  experts, which account for  $(2 + 1) \times 6 + 1 = 19$  tunable prompts in total per-layer. We increase the number of  $k$ , and at each step we also report the result of increasing  $l$  in vanilla prompt to the same total number of prompts. The results are summarized in Fig. 4.

As illustrated in the figure, adding the MoPE design with as few as  $k = 2$  experts boosts performance, and increasing the number of experts leads to a monotonic performance improvement which avoids over-length deterioration. In contrast, length-scaling does not lead to a linear performance improvement and is prone to performance deterioration, which is consistent with previous findings (Jia et al. 2022; Yang et al. 2022a; Khattak et al. 2023; Li and Liang 2021). Additionally, longer prompts in vanilla prompt tuning can exacerbate computational overhead due to the quadratic time complexity of self-attention. This is why we cannot experiment with  $l > 199$  for the other two methods. By con-

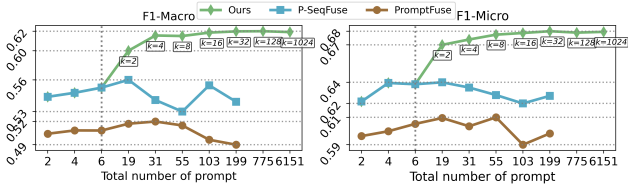


Figure 4: **More experts v.s. longer prompts.** We compare increasing the number of experts,  $k$ , versus lengthen prompt,  $l$ . Expert-scaling consistently outperforms length-scaling, exhibiting a linear growth trend and do not deteriorate even when  $k \rightarrow \infty$ . Conversely, excessive prompt length has a negative impact on accuracy and speed.

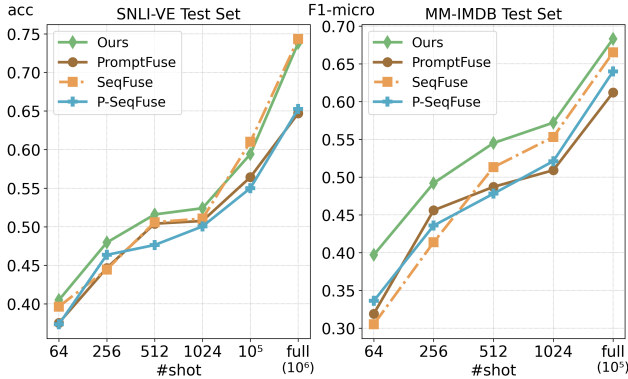


Figure 5: **Scaling performance with increased training data.** We show the performance of our method and representative methods as we progressively increase the amount of training data, or “#shots”. Our method outperform other prompt fusion methods at all data scales.

trast, MoPE scales by conditioning the dynamic prompt on more experts while maintaining a fixed prompt length during actual self-attention. As a result, our method maintains a nearly constant time complexity.

**MoPE scales better with more training data.** Previous prompting methods have been shown to not scale well with respect to increased training data (Gao et al. 2022; Liang, Zhao, and Schütze 2022; Tsimpoukelli et al. 2021; Yang et al. 2022a). To assess the scalability of MoPE, we subsample the training set with different shots to simulate a range of low-shot to high-shot learning scenarios. We then train our method and other prompt-tuning and fine-tuning methods on the same subset of SNLI-VE and MM-IMDB.

As Fig. 5 shows, our MoPE-based method demonstrates superior scalability compared to other prompt tuning methods. Specifically, we consistently match the results of the fine-tuning method, *SeqFuse*, on the SNLI-VE dataset, while surpassing it on the MM-IMDB dataset. By contrast, the methods based on vanilla prompts do not scale well with respect to increased training data, resulting in a consistent performance gap between our method and the compared methods. This performance disparity becomes more pronounced on larger datasets, such as when training with

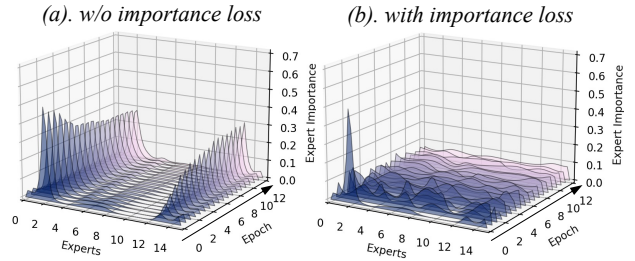


Figure 6: **Effect of the importance loss.** We visualize how the importance (z-axis) of all experts (x-axis) in the last Transformer layer changes during training (y-axis). (a) Without importance loss, only a few experts are used throughout training (b) The importance loss ensures balanced utilization of all experts.

Routing Embed	SNLI-VE $\uparrow$	UPMC Food $\uparrow$	MM-IMDB $\uparrow$
Frozen	73.55	91.74	62.01/68.25
Learned	73.13	91.20	61.64/67.97

Table 4: **Result of frozen routing embedding.** Frozen routing embedding are slightly better than learned one.

$10^5$  shots or using the full training set.

**Frozen routing embedding outperform learned embedding.** We ablate the effect of using frozen routing embeddings. As Tab. 4 shows, fixed routing embedding could achieve the same result as the trained one.

**Importance loss aids expert specialization.** The importance loss is crucial for avoiding degenerate routing solutions and, consequently, aids expert specialization. In Fig. 6, we visualize how the importance (i.e., average routing score) of each expert changes when training on the SNLI-VE dataset. Without the importance loss, routing adheres to its initial state, resulting in a skewed distribution where a few experts are always being routed. Adding it aids expert specialization by penalizing highly unbalanced expert importance.

**How MoPE could be more expressive.** We have demonstrated that the proposed MoPE scales better with trainable parameters and data. This increased expressiveness comes from two factors. First, previous methods use a shared prompt for all instances and neglect multimodal interplay. By contrast, our dynamic prompt with MoPE is adaptive, and finding an instance-wise optimal prompt can lead to better results. Secondly, MoPE circumvents the challenge of optimizing a long prompt (Petrov, Torr, and Bibi 2023). By doing so, we shift the difficulty from learning a universal long prompt to learning a parameterized router with multiple short prompts. As a result, our empirical expressiveness is closer to the theoretical upper bound of prompt tuning.

## Conclusion

In this paper, we propose an adaptive and expressive prompt-based method for fusing unimodal models. Our method involves decomposing the prompt for instance-adaptive

prompt learning. To effectively scale up the prompt while avoiding performance deterioration, we introduce MoPE, which improves the expressiveness of prompt tuning. Extensive experiments demonstrate that our method is highly parameter-efficient and scales better with dataset size and prompt length. We believe MoPE could be an efficient fusion method for a wide array of multimodal tasks.

## References

- Arevalo, J.; Solorio, T.; Montes-y Gómez, M.; and González, F. A. 2017. Gated multimodal units for information fusion. *arXiv preprint arXiv:1702.01992*.
- Baevski, A.; Zhou, Y.; Mohamed, A.; and Auli, M. 2020. wav2vec 2.0: A framework for self-supervised learning of speech representations. *Advances in neural information processing systems*, 33: 12449–12460.
- Bahng, H.; Jahanian, A.; Sankaranarayanan, S.; and Isola, P. 2022. Exploring visual prompts for adapting large-scale models. *arXiv preprint arXiv:2203.17274*.
- Castro, S.; Hazarika, D.; Pérez-Rosas, V.; Zimmermann, R.; Mihalcea, R.; and Poria, S. 2019. Towards multimodal sarcasm detection (an \_obviously\_ perfect paper). *arXiv preprint arXiv:1906.01815*.
- Devlin, J.; Chang, M.-W.; Lee, K.; and Toutanova, K. 2018. Bert: Pre-training of deep bidirectional transformers for language understanding. *arXiv preprint arXiv:1810.04805*.
- Dosovitskiy, A.; Beyer, L.; Kolesnikov, A.; Weissenborn, D.; Zhai, X.; Unterthiner, T.; Dehghani, M.; Minderer, M.; Heigold, G.; Gelly, S.; et al. 2020. An image is worth 16x16 words: Transformers for image recognition at scale. *arXiv preprint arXiv:2010.11929*.
- Eigen, D.; Ranzato, M.; and Sutskever, I. 2013. Learning factored representations in a deep mixture of experts. *arXiv preprint arXiv:1312.4314*.
- Fedus, W.; Zoph, B.; and Shazeer, N. 2022. Switch transformers: Scaling to trillion parameter models with simple and efficient sparsity. *The Journal of Machine Learning Research*, 23(1): 5232–5270.
- Gao, Y.; Shi, X.; Zhu, Y.; Wang, H.; Tang, Z.; Zhou, X.; Li, M.; and Metaxas, D. N. 2022. Visual prompt tuning for test-time domain adaptation. *arXiv preprint arXiv:2210.04831*.
- Goyal, Y.; Khot, T.; Summers-Stay, D.; Batra, D.; and Parikh, D. 2017. Making the v in vqa matter: Elevating the role of image understanding in visual question answering. In *Proceedings of the IEEE conference on computer vision and pattern recognition*, 6904–6913.
- Jia, M.; Tang, L.; Chen, B.-C.; Cardie, C.; Belongie, S.; Hariharan, B.; and Lim, S.-N. 2022. Visual prompt tuning. In *European Conference on Computer Vision*, 709–727. Springer.
- Jiang, R.; Liu, L.; and Chen, C. 2023. Clip-count: Towards text-guided zero-shot object counting. In *Proceedings of the 31st ACM International Conference on Multimedia*, 4535–4545.
- Kazemzadeh, S.; Ordonez, V.; Matten, M.; and Berg, T. 2014. Referitgame: Referring to objects in photographs of natural scenes. In *Proceedings of the 2014 conference on empirical methods in natural language processing (EMNLP)*, 787–798.
- Khattak, M. U.; Rasheed, H.; Maaz, M.; Khan, S.; and Khan, F. S. 2023. Maple: Multi-modal prompt learning. In *Proceedings of the IEEE/CVF Conference on Computer Vision and Pattern Recognition*, 19113–19122.
- Kiela, D.; Bhooshan, S.; Firooz, H.; Perez, E.; and Tegg, D. 2019. Supervised multimodal bitransformers for classifying images and text. *arXiv preprint arXiv:1909.02950*.
- Kim, Y.; Li, Y.; Moitra, A.; and Panda, P. 2023. Do We Really Need a Large Number of Visual Prompts? *arXiv preprint arXiv:2305.17223*.
- Lepikhin, D.; Lee, H.; Xu, Y.; Chen, D.; Firat, O.; Huang, Y.; Krikun, M.; Shazeer, N.; and Chen, Z. 2020. Gshard: Scaling giant models with conditional computation and automatic sharding. *arXiv preprint arXiv:2006.16668*.
- Lester, B.; Al-Rfou, R.; and Constant, N. 2021. The power of scale for parameter-efficient prompt tuning. *arXiv preprint arXiv:2104.08691*.
- Li, X. L.; and Liang, P. 2021. Prefix-tuning: Optimizing continuous prompts for generation. *arXiv preprint arXiv:2101.00190*.
- Li, Y.; Quan, R.; Zhu, L.; and Yang, Y. 2023. Efficient Multimodal Fusion via Interactive Prompting. In *Proceedings of the IEEE/CVF Conference on Computer Vision and Pattern Recognition*, 2604–2613.
- Liang, S.; Zhao, M.; and Schütze, H. 2022. Modular and parameter-efficient multimodal fusion with prompting. *arXiv preprint arXiv:2203.08055*.
- Lin, J.; Chang, J.; Liu, L.; Li, G.; Lin, L.; Tian, Q.; and Chen, C.-w. 2023. Being comes from not-being: Open-vocabulary text-to-motion generation with wordless training. In *Proceedings of the IEEE/CVF conference on computer vision and pattern recognition*, 23222–23231.
- Liu, L.; Chang, J.; Yu, B. X.; Lin, L.; Tian, Q.; and Chen, C.-W. 2022. Prompt-matched semantic segmentation. *arXiv preprint arXiv:2208.10159*.
- Liu, X.; Ji, K.; Fu, Y.; Tam, W. L.; Du, Z.; Yang, Z.; and Tang, J. 2021a. P-tuning v2: Prompt tuning can be comparable to fine-tuning universally across scales and tasks. *arXiv preprint arXiv:2110.07602*.
- Liu, Z.; Lin, Y.; Cao, Y.; Hu, H.; Wei, Y.; Zhang, Z.; Lin, S.; and Guo, B. 2021b. Swin transformer: Hierarchical vision transformer using shifted windows. In *Proceedings of the IEEE/CVF international conference on computer vision*, 10012–10022.
- Loshchilov, I.; and Hutter, F. 2017. Decoupled weight decay regularization. *arXiv preprint arXiv:1711.05101*.
- Mustafa, B.; Riquelme, C.; Puigcerver, J.; Jenatton, R.; and Hounsby, N. 2022. Multimodal contrastive learning with limoe: the language-image mixture of experts. *Advances in Neural Information Processing Systems*, 35: 9564–9576.

- Petrov, A.; Torr, P. H.; and Bibi, A. 2023. When Do Prompting and Prefix-Tuning Work? A Theory of Capabilities and Limitations. *arXiv preprint arXiv:2310.19698*.
- Qin, G.; and Eisner, J. 2021. Learning how to ask: Querying LMs with mixtures of soft prompts. *arXiv preprint arXiv:2104.06599*.
- Radford, A.; Wu, J.; Child, R.; Luan, D.; Amodei, D.; Sutskever, I.; et al. 2019. Language models are unsupervised multitask learners. *OpenAI blog*, 1(8): 9.
- Riquelme, C.; Puigcerver, J.; Mustafa, B.; Neumann, M.; Jenatton, R.; Susano Pinto, A.; Keysers, D.; and Houlsby, N. 2021. Scaling vision with sparse mixture of experts. *Advances in Neural Information Processing Systems*, 34: 8583–8595.
- Saxe, A. M.; McClelland, J. L.; and Ganguli, S. 2013. Exact solutions to the nonlinear dynamics of learning in deep linear neural networks. *arXiv preprint arXiv:1312.6120*.
- Shazeer, N.; Mirhoseini, A.; Maziarz, K.; Davis, A.; Le, Q.; Hinton, G.; and Dean, J. 2017. Outrageously large neural networks: The sparsely-gated mixture-of-experts layer. *arXiv preprint arXiv:1701.06538*.
- Tsimpoukelli, M.; Menick, J. L.; Cabi, S.; Eslami, S.; Vinyals, O.; and Hill, F. 2021. Multimodal few-shot learning with frozen language models. *Advances in Neural Information Processing Systems*, 34: 200–212.
- Vaswani, A.; Shazeer, N.; Parmar, N.; Uszkoreit, J.; Jones, L.; Gomez, A. N.; Kaiser, Ł.; and Polosukhin, I. 2017. Attention is all you need. *Advances in neural information processing systems*, 30.
- Wang, X.; Kumar, D.; Thome, N.; Cord, M.; and Precioso, F. 2015. Recipe recognition with large multimodal food dataset. In *2015 IEEE International Conference on Multimedia & Expo Workshops (ICMEW)*, 1–6. IEEE.
- Wang, Y.; Chauhan, J.; Wang, W.; and Hsieh, C.-J. 2023. Universality and Limitations of Prompt Tuning. *arXiv preprint arXiv:2305.18787*.
- Xie, N.; Lai, F.; Doran, D.; and Kadav, A. 2019. Visual entailment: A novel task for fine-grained image understanding. *arXiv preprint arXiv:1901.06706*.
- Yang, H.; Lin, J.; Yang, A.; Wang, P.; Zhou, C.; and Yang, H. 2022a. Prompt tuning for generative multimodal pretrained models. *arXiv preprint arXiv:2208.02532*.
- Yang, Z.; Gan, Z.; Wang, J.; Hu, X.; Lu, Y.; Liu, Z.; and Wang, L. 2022b. An empirical study of gpt-3 for few-shot knowledge-based vqa. In *Proceedings of the AAAI Conference on Artificial Intelligence*, volume 36, 3081–3089.
- Zheng, S.; Lu, J.; Zhao, H.; Zhu, X.; Luo, Z.; Wang, Y.; Fu, Y.; Feng, J.; Xiang, T.; Torr, P. H.; et al. 2021. Rethinking semantic segmentation from a sequence-to-sequence perspective with transformers. In *Proceedings of the IEEE/CVF conference on computer vision and pattern recognition*, 6881–6890.
- Zhou, K.; Yang, J.; Loy, C. C.; and Liu, Z. 2022a. Conditional prompt learning for vision-language models. In *Proceedings of the IEEE/CVF Conference on Computer Vision and Pattern Recognition*, 16816–16825.
- Zhou, K.; Yang, J.; Loy, C. C.; and Liu, Z. 2022b. Learning to prompt for vision-language models. *International Journal of Computer Vision*, 130(9): 2337–2348.

## Additional Details on Experiments

In this section, we provide additional details on our model architecture, experimental setup, and data preprocessing.

### Architecture Details

**Prompt Vector.** Our prompt implementation closely follows VPT (Jia et al. 2022). Specifically, for static prompts and prompt experts, we use uniform initialization  $\mathcal{U} \sim (-\eta, \eta)$ , where  $\eta$  is calculated according to the embedding dimension and patch size of the Transformer (Jia et al. 2022). Dropout with  $p = 0.1$  is applied to all prompts. However, we do not use the reparameterization trick for prompts introduced in the original prompt tuning methods (Li and Liang 2021), as the gradients of our dynamic prompt and mapped prompt are already rectified by MLPs (i.e.,  $\mathbf{W}_x, \mathbf{W}_y, f_m(\cdot)$ ). For Transformer architectures that employ a window attention mechanism (e.g., Swin (Liu et al. 2021b)), we duplicate the same prompt and prepend it to all windows for self-attention calculation, following the approach in VPT (Jia et al. 2022).

**Mapper.** We learn a mapper to map representations from complementary modality  $\mathbb{Y}$  to the embedding dimension of main modality  $\mathbb{X}$ . Generally speaking, the mapper is implemented as a two-layer MLP with a bottleneck design, which shares similarities with previous work (Li et al. 2023). In our experiments, we set the bottleneck dimension as half of the dimension of the complementary representation, i.e.,  $d_{bot} = \lceil d_y/2 \rceil$ . Then, we apply a batch normalization layer and a GeLU activation to obtain a bottleneck feature  $\psi_{bot} \in \mathbb{R}_{d_{bot}}$ .

After obtaining this bottleneck feature, we apply another linear layer to project it to the dimension of  $d_x$ . However, some Transformer architectures use inconsistent  $d_x$  in different layers. For example, in Swin-b (Liu et al. 2021b), the embedding dimension changes from [128, 256, 512, 1024], making it challenging to fit a single linear transformation. To circumvent this, we instead learn four separate linear projections, each used to project the shared bottleneck feature to different embedding dimensions. As a result, there is one single down-sampling layer and multiple up-sampling layers. The design is illustrated in Fig 7. **MoPE.** As discussed in the main body of this paper, we learn a per-layer linear projection  $\mathbf{W}_x^i$  to obtain the cross-modal embedding. Here, we would like to further clarify that the weight is not shared with the one used in the mapper  $f_m$ . In our experiments, we use  $d_c = 8$  and  $d_i = 2$ , resulting in  $d_r = 10$ . The ablation on the two dimensions can be found in the second part of this supplementary material. For the importance loss, we scale it by a factor of 0.01 and linearly combine it with the task-specific loss(es) for optimization.

### Dataset

**UPMC Food-101** (Wang et al. 2015) serves as a comprehensive multimodal dataset designed for fine-grained recipe classification. The dataset contains 90,840 image-text pairs for 101 food classes. We follow previous methods (Li et al. 2023; Kiela et al. 2019) to create a validation set of 5000 samples.

**MM-IMDB** (Arevalo et al. 2017) is a multimodal movie classification dataset. It comprises 25,956 pairs of images

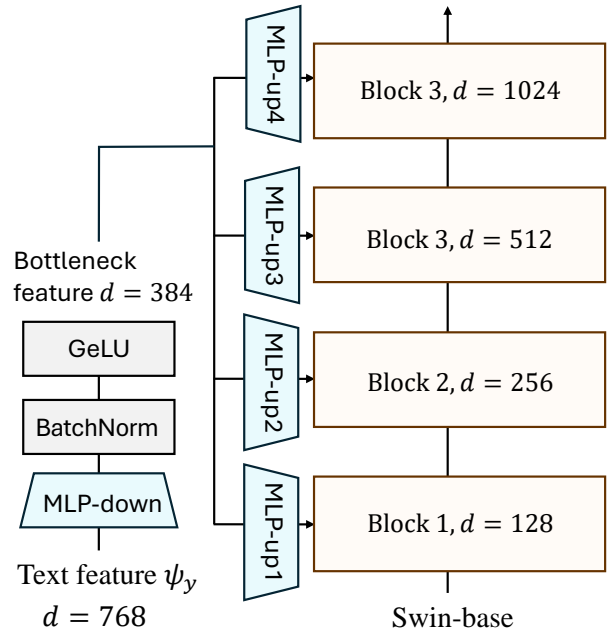


Figure 7: **Architecture of the Mapper for Swin.** The cross model feature is first projected to a low-dimensional bottleneck, then further mapped to different embedding dimension of each Swin blocks.

and texts, each pair including a movie poster and a plot summary. The dataset supports multi-label genre classification across a spectrum of 23 genres with highly imbalanced classes.

**SNLI-VE** (Xie et al. 2019) is a large-scale multimodal dataset with 565,286 image-text pairs. The task for this dataset is visual entailment, which means that the model should decide whether a hypothesis matches the given premise or not. This dataset provide image and text premise, while the hypothesis is always in text modality.

**MUStARD** (Castro et al. 2019) is a dataset for multimodal sarcasm detection. The original dataset contains 690 video clips in MP4 format with an even number of sarcastic and non-sarcastic labels. Each video is provided with annotations in the language modality, describing the speaker and sentence in that video. Collectively, there are three modalities available: video, audio extracted from the video, and the language modality.

**RefCOCO** and **RefCOCO+** (Kazemzadeh et al. 2014) are two datasets for referring image segmentation. Both datasets are built based on MSCOCO and contain around 19,900 images with 50,000 objects and 140,000 referring expressions. RefCOCO allows referring expressions of any type, while RefCOCO+ features expressions that do not contain object positions.

In Fig. 8, we provide examples of each dataset.

### Data Processing

For all input images, we perform RandAug with  $N = 2$  and  $M = 5$ , resize them to (256, 256), and perform center

Dataset	Image (Video)	Text	label
SNLI-VE		A young child wearing an overall dress with a floral patterned skirt and a white t-shirt pets a baby deer with a backpack on her back.	entailment
UPMC Food 101		Skip to Main Content * All You * Coastal Living * Cooking Light * Food and Wine * Health * My Recipes * Real Simple * Southern Living * Sunset Search MyRecipes.com ...	Apple pie
MM-IMDB		Susie, a plain young country girl, secretly loves a neighbor boy, William. She believes in him and sacrifices much of her own happiness to promote his own ambitions, all without his knowledge. Eventually he rises to a position of success ...	Comedy Drama Romance
MuSTARD		Well, he said it was a tribble. It could be a toupee, but either way, it's pretty cool.	Sarcasm: False
RefCOCO		The catcher	

Figure 8: Examples of each dataset used in the main paper.

cropping to obtain images of size (224, 224).

For the SNLI-VE dataset, we follow Frozen and PMF and use only the image premise, which means that the input to the model is the image premise + text hypothesis. Note that this setting may differ from other works that also use the text premise.

For the MuSTARD dataset, the overall processing pipeline follows PromptFuse (Liu et al. 2022). For the audio modality, we extract WAV audio from the video using a sampling rate of 16,000 Hz. We also remove background noise using the Librosa package. For a batch of input, we zero-pad the WAV input to the same length. As for the video, while PromptFuse (Liu et al. 2022) uses a face detection model to only sample frames where the speaker’s face is visible,

we evenly sample 8 frames for all videos in time. The sampled frames are resized to (224, 224) for encoding. For the text modality, we use the speaker-dependent setting, which means that the speaker’s name is visible to the model during both training and inference. To achieve this, we simply concatenate the speaker’s name to the input utterance string.

## Extended Analysis and Discussion

This section aims to provide further ablation study on the design choices and hyper-parameters. We also provided extended discussion on the effectiveness of proposed MoPE.

## Additional Ablations

**Ablation on dimension of  $d_i$  and  $d_c$ .** Our finding indicate that  $d_c \gg d_i$  results in better performance in general, and we set  $d_c = 8, d_i = 2$  in our main experiment as ablated in Tab. 5.

$k = 4$	$d_i = 10, d_c = 0$	$d_i = 8, d_c = 2$	$d_i = 5, d_c = 5$	$d_i = 2, d_c = 8$	$d_i = 0, d_c = 10$
MM-IMDB( $\uparrow$ )	54.50/64.63	60.12/67.02	61.22/67.51	<b>61.93/68.19</b>	60.91/67.93

Table 5: **Ablation on  $d_c$  and  $d_i$ .**  $d_c \gg d_i$  is better.

**Ablation on vision encoder.** In main experiment we use swin-base as the vision encoder. To have a fair comparison on previous prompt fusion methods (Li et al. 2023; Liang, Zhao, and Schütze 2022) that are based on ViT (Dosovitskiy et al. 2020), we provide the result of our method with ViT-base as vision encoder in Tab. 6, with results measured using 3 random seeds, As the table shows, using the ViT as vision encoder gives similar results. The result demonstrate that our superior performance is not due to more advanced vision encoder.

Method	Param	SNLI-VE( $\uparrow$ )	UPMC Food( $\uparrow$ )	MM-IMDB( $\uparrow$ )
Ours(ViT-B)	1.6M	73.47 $\pm$ .11	91.55 $\pm$ .12	62.37 $\pm$ .35/68.73 $\pm$ .24
Ours(Swin-B)	1.6M	73.14 $\pm$ .21	91.54 $\pm$ .21	61.93 $\pm$ .37/68.19 $\pm$ .14

Table 6: **Ablation on ViT as the main vision encoder.**

## Analysis on Adaptivity of Vanilla Prompt and MoPE

In the main body of the paper, we have empirically demonstrated that the dynamic prompt generated by MoPE exhibits greater adaptivity compared to global-shared prompt tuning. In this section, we aim to further characterize and quantify the adaptiveness of different prompt techniques. Through this analysis, we will also provide intuitive insights into the significance of expert specialization in MoPE-based fusion.

Following the approach adopted in previous papers (Wang et al. 2023; Petrov, Torr, and Bibi 2023), we will focus our analysis on the case of a single prompt within a single Transformer layer. Since our method is designed to generate an effective prompt while leaving the attention calculation the same as previous prompt tuning, our MoPE will only affect the forward behavior up to the calculation of attention map. Therefore, we will concentrate on analyzing how different prompts influence the attention pattern of a pretrained Transformer layer.

Let us define the attention map produced by the self-attention operation as  $\mathbf{A}(\mathbf{X}, \mathbf{P})$ , which is a function of the input  $\mathbf{X}$  and the prompt  $\mathbf{P}$ . The objective is to find a prompt  $\mathbf{P}$  that enables the attention map  $\mathbf{A}(\mathbf{X}, \mathbf{P})$  to closely match the desired target attention pattern for each input instance.

### Theorem 1 (Limited Adaptivity of Global-shared Prompt)

Let  $\mathcal{X}$  be the input space, and  $\mathcal{A}$  be the space of attention matrices. For any input  $\mathbf{x} \in \mathcal{X}$ , let  $\mathcal{A}^*(\mathbf{x}) \subseteq \mathcal{A}$  denote the set of optimal attention patterns that minimize the downstream task loss. Define the attention mapping induced by a prompt  $\mathbf{P}$  as  $\mathcal{A}(\mathbf{x}, \mathbf{P}) \subseteq \mathcal{A}$ . Then, for vanilla prompting

with a single shared prompt  $\mathbf{P}$ , there exists no  $\mathbf{P} \in \mathcal{P}$  such that  $\mathcal{A}^*(\mathbf{x}) \subseteq \mathcal{A}(\mathbf{x}, \mathbf{P})$  for all  $\mathbf{x} \in \mathcal{X}$ , where  $\mathcal{P}$  is the prompt space.

**Proof.1** Let  $\mathbf{x}_1, \mathbf{x}_2 \in \mathcal{X}$  be two distinct input instances with disjoint optimal attention sets, i.e.,  $\mathcal{A}^*(\mathbf{x}_1) \cap \mathcal{A}^*(\mathbf{x}_2) = \emptyset$ . Define the attention discrepancy for an instance  $\mathbf{x}$  and prompt  $\mathbf{P}$  as:

$$\Delta(\mathbf{x}, \mathbf{P}) = \inf_{\mathbf{A} \in \mathcal{A}(\mathbf{x}, \mathbf{P})} \|\mathbf{A} - \mathcal{A}^*(\mathbf{x})\|_{\mathcal{A}} \quad (6)$$

where  $\|\cdot\|_{\mathcal{A}}$  is a suitable distance metric on  $\mathcal{A}$ .

Let  $\mathbf{P}_1^*$  and  $\mathbf{P}_2^*$  be the locally optimal prompts for instances  $\mathbf{x}_1$  and  $\mathbf{x}_2$ , respectively, i.e.,

$$\mathbf{P}_1^* = \arg \min_{\mathbf{P} \in \mathcal{P}} \Delta(\mathbf{x}_1, \mathbf{P}) \quad (7)$$

$$\mathbf{P}_2^* = \arg \min_{\mathbf{P} \in \mathcal{P}} \Delta(\mathbf{x}_2, \mathbf{P}) \quad (8)$$

For vanilla prompting with a shared prompt  $\mathbf{P}$ , the globally optimal shared prompt  $\mathbf{P}_{shared}^*$  minimizes the accumulated attention discrepancy:

$$\mathbf{P}_{shared}^* = \arg \min_{\mathbf{P} \in \mathcal{P}} \Delta(\mathbf{x}_1, \mathbf{P}) + \Delta(\mathbf{x}_2, \mathbf{P}) \quad (9)$$

Due to the disjointness of optimal attention sets for each instance, the accumulated attention discrepancy for the globally optimal shared prompt  $\mathbf{P}_{shared}^*$  is lower-bounded by the sum of the locally optimal attention discrepancies for  $\mathbf{x}_1$  and  $\mathbf{x}_2$ :

$$\Delta(\mathbf{x}_1, \mathbf{P}_{shared}^*) + \Delta(\mathbf{x}_2, \mathbf{P}_{shared}^*) \geq \Delta(\mathbf{x}_1, \mathbf{P}_1^*) + \Delta(\mathbf{x}_2, \mathbf{P}_2^*) \quad (10)$$

Furthermore, by the limited expressiveness of prompt-tuning (Petrov, Torr, and Bibi 2023), we have:

$$\Delta(\mathbf{x}_2, \mathbf{P}_2^*) \geq 0; \Delta(\mathbf{x}_1, \mathbf{P}_1^*) \geq 0 \quad (11)$$

Hence, the following relationship holds:

$$\Delta(\mathbf{x}_1, \mathbf{P}_{shared}^*) + \Delta(\mathbf{x}_2, \mathbf{P}_{shared}^*) \geq \Delta(\mathbf{x}_1, \mathbf{P}_1^*) + \Delta(\mathbf{x}_2, \mathbf{P}_2^*) \geq 0 \quad (12)$$

**Theorem 2 (Improved Adaptivity of MoPE)** Let  $\mathcal{E} = \{\mathcal{E}_1, \mathcal{E}_2, \dots, \mathcal{E}_k\}$  be a set of  $k$  expert attention mappings, where each  $\mathcal{E}_i : \mathcal{X} \rightarrow \mathcal{A}$  maps an input  $\mathbf{x} \in \mathcal{X}$  to a set of attention patterns  $\mathcal{E}_i(\mathbf{x}) \subseteq \mathcal{A}$ . Define the induced attention mapping of MoPE as:

$$\mathcal{A}_{MoPE}(\mathbf{x}, \mathcal{E}, \mathbf{r}) = \left\{ \sum_{i=1}^k r_i(\mathbf{x}) \mathbf{A}_i \mid \mathbf{A}_i \in \mathcal{E}_i(\mathbf{x}), \forall i \right\} \quad (13)$$

where  $\mathbf{r}(\mathbf{x}) = [r_1(\mathbf{x}), \dots, r_k(\mathbf{x})]$  are the routing weights for input  $\mathbf{x}$ .

Let  $\mathcal{X}' \subseteq \mathcal{X}$  be a set of instances. If the convex hull of the expert attention mappings, denoted as:

$$\text{conv}(\mathcal{E}) = \left\{ \sum_{i=1}^k \alpha_i \mathbf{A}_i \mid \mathbf{A}_i \in \mathcal{E}_i(\mathbf{x}), \forall i, \forall \mathbf{x} \in \mathcal{X}', \sum_{i=1}^k \alpha_i = 1, \alpha_i \geq 0 \right\} \quad (14)$$

contains an optimal attention pattern for each instance in  $\mathcal{X}'$ , i.e.,  $\mathcal{A}^*(\mathbf{x}) \subseteq \text{conv}(\mathcal{E}), \forall \mathbf{x} \in \mathcal{X}'$ , then there exists a routing score  $\mathbf{r}^*$  such that the accumulated attention discrepancy for MoPE under  $\mathbf{r}^*$  across instances in  $\mathcal{X}'$  is equal to the sum of the optimal instance-wise attention discrepancies, i.e.,

$$\sum_{\mathbf{x} \in \mathcal{X}'} \Delta(\mathbf{x}, \mathcal{E}, \mathbf{r}^*) = \sum_{\mathbf{x} \in \mathcal{X}'} \inf_{\mathbf{A} \in \mathcal{A}^*(\mathbf{x})} \|\mathbf{A} - \mathbf{A}^*\|_{\mathcal{A}} \quad (15)$$

**Proof .2** When there are more experts than instances, i.e.,  $|\mathcal{X}'| \leq k$ , the proof is trivial. This is because the optimal prompt for each instance could simply be “stored” in one or a few experts.

When cardinality of the instances is greater than the number of experts, i.e.,  $|\mathcal{X}'| > k$ . Let  $\mathcal{X}' \subseteq \mathcal{X}$  be a set of instances with  $|\mathcal{X}'| > k$ , and assume that the convex hull of the expert attention mappings,  $\text{conv}(\mathcal{E})$ , contains an optimal attention pattern for each instance in  $\mathcal{X}'$ , i.e.,  $\mathcal{A}^*(\mathbf{x}) \subseteq \text{conv}(\mathcal{E}), \forall \mathbf{x} \in \mathcal{X}'$ . We call this premise as the specialized experts condition.

Since the routing weights  $\mathbf{r}(\mathbf{x})$  are convex combinations of the expert attention patterns, the induced attention mapping of MoPE,  $\mathcal{A}_{\text{MoPE}}(\mathbf{x}, \mathcal{E}, \mathbf{r})$ , is equal to  $\text{conv}(\mathcal{E})$ :

$$\mathcal{A}_{\text{MoPE}}(\mathbf{x}, \mathcal{E}, \mathbf{r}) = \text{conv}(\mathcal{E}), \quad \forall \mathbf{x} \in \mathcal{X}' \quad (16)$$

Therefore, for each instance  $\mathbf{x} \in \mathcal{X}'$ , there exists an attention pattern  $\mathbf{A}^* \in \mathcal{A}^*(\mathbf{x})$  that is also contained in  $\mathcal{A}_{\text{MoPE}}(\mathbf{x}, \mathcal{E}, \mathbf{r}^*)$  for some routing score  $\mathbf{r}^*$ , i.e.,

$$\exists \mathbf{A}^* \in \mathcal{A}^*(\mathbf{x}) \cap \mathcal{A}_{\text{MoPE}}(\mathbf{x}, \mathcal{E}, \mathbf{r}^*), \quad \forall \mathbf{x} \in \mathcal{X}' \quad (17)$$

This implies that the attention discrepancy for each instance  $\mathbf{x} \in \mathcal{X}'$  under the routing score  $\mathbf{r}^*$  is equal to the optimal instance-wise attention discrepancy:

$$\begin{aligned} \Delta(\mathbf{x}, \mathcal{E}, \mathbf{r}^*) &= \inf_{\mathbf{A} \in \mathcal{A}_{\text{MoPE}}(\mathbf{x}, \mathcal{E}, \mathbf{r}^*)} \|\mathbf{A} - \mathbf{A}^*\|_{\mathcal{A}} \\ &= \inf_{\mathbf{A} \in \mathcal{A}^*(\mathbf{x})} \|\mathbf{A} - \mathbf{A}^*\|_{\mathcal{A}}, \quad \forall \mathbf{x} \in \mathcal{X}' \end{aligned} \quad (18)$$

Therefore, the accumulated attention discrepancy for MoPE under the routing score  $\mathbf{r}^*$  across instances in  $\mathcal{X}'$  is equal to the sum of the optimal instance-wise attention discrepancies:

$$\sum_{\mathbf{x} \in \mathcal{X}'} \Delta(\mathbf{x}, \mathcal{E}, \mathbf{r}^*) = \sum_{\mathbf{x} \in \mathcal{X}'} \inf_{\mathbf{A} \in \mathcal{A}^*(\mathbf{x})} \|\mathbf{A} - \mathbf{A}^*\|_{\mathcal{A}} \quad (19)$$

which is equivalent as:

$$\sum_{\mathbf{x} \in \mathcal{X}'} \Delta(\mathbf{x}, \mathcal{E}, \mathbf{r}^*) = \sum_{\mathbf{x} \in \mathcal{X}'} \Delta(\mathbf{x}, \mathbf{P}_{\mathbf{x}}^*) \geq 0 \quad (20)$$

Thus, when the number of instances exceeds the number of experts, if the convex hull of the expert attention mappings contains an optimal attention pattern for each instance, then there exists a routing score  $\mathbf{r}^*$  that allows MoPE to achieve an accumulated attention discrepancy equal to the sum of the optimal instance-wise attention discrepancies across those instances.

Putting it together, the Theorem. 1 state that the global-shared prompt (i.e., vanilla prompt) could not achieve the best result, when the input instances require different attention patterns to perform well. Theorem. 2 state that it is possible for MoPE to achieve the best result on all of the input instances, conditioned on the appropriate specialization of experts.

## Discussion: How to Choose the Main Modality?

In the proposed method, we use a sequential pipeline to fuse different modalities. In this pipeline, the input of the complementary modality  $\mathbb{Y}$  is first encoded into a representation  $\psi_y$ , which is then used to guide the prompting of modality  $\mathbb{X}$ . This design raises an interesting question: “How to choose the complementary and main modality?”

For tasks that do not require a dense representation, such as classification, our experience is that either modality can be used as the main modality, yielding similar results. In our experiments, we utilize vision as the main modality due to empirically better results, but this does not necessarily mean that the text encoder cannot be the main modality. We have also tested using text as the main modality, and the results are summarized in Tab. 7.

Method	SNLI-VE	Food-101	MM-IMDB
Ours(LM)	71.10±.12	88.01±.12	58.38±.11/65.81±.23
Ours(VM)	73.59±.15	92.05±.11	62.01±.21/68.24±.12

Table 7: Result of Language Model (LM) as main modality.

As the table shows, using BERT as the main encoder results in a decline in performance. Our postulation is that for these three tasks, the text input contains a significant amount of noisy and false positive data. For instance, in the UPMC-Food 101 dataset (Wang et al. 2015), the text data is derived using a spider, which includes many irrelevant hypertext and website titles. Therefore, treating the text as the main modality can lead to overfitting and biased predictions.

For tasks that require a modality-specific dense representation for decoding, the main modality must be the one that provides such output for compatibility. For example, in referring expression segmentation, we have to use the image as main modality, because the segmentation head expects feature maps instead of a global representation.

## Our MoPE-based method yields a better multimodal representation.

We visualize the multimodal representation generated by different methods using t-SNE. For *LateConcat*, this would be the concatenated feature from both modalities. For the other methods, we visualize the [CLS] token of the main modality. For ease of coloring, we only show the first 20 classes in the test set of the UPMC Food-101 (Wang et al. 2015) dataset. The results are presented in Fig. 9. As the results show, the representation generated by our method is the most separable.

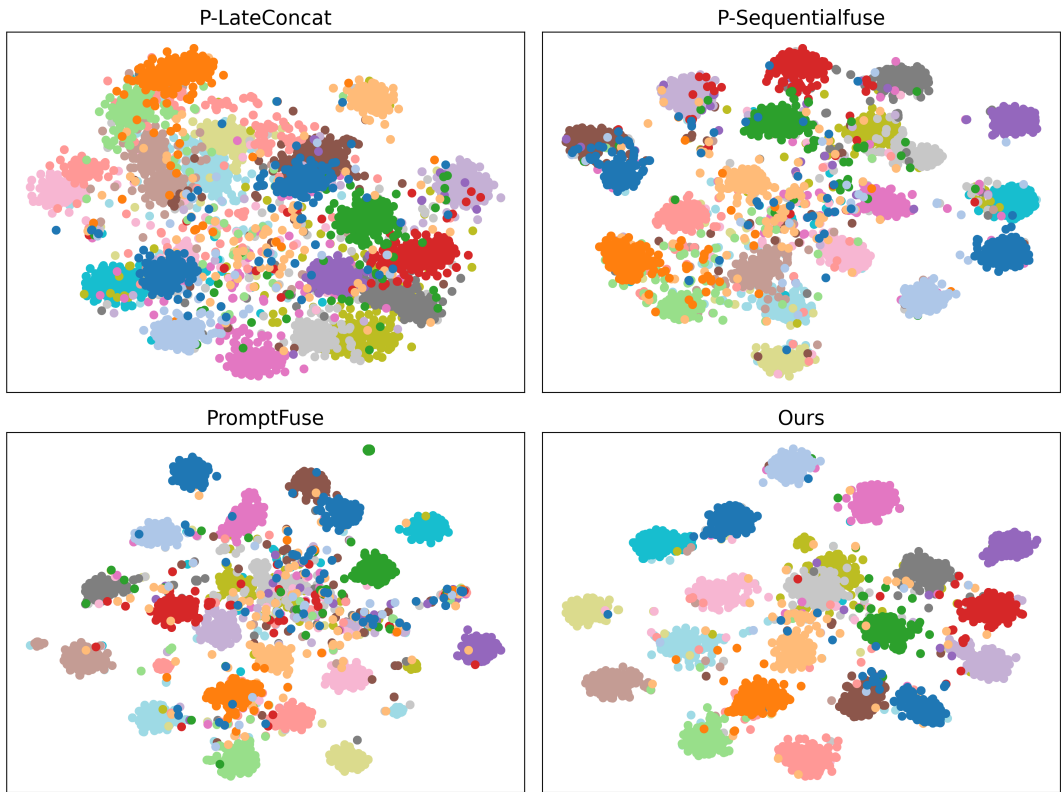


Figure 9: **t-SNE visualization of multimodal representation generated by different methods.** The representation generated by our method is the most separable. Better viewed with color.

## Additional Visualizations

### Visualization of Referring Expression Segmentation Results

In Fig. 10, Fig. 11 we provide a qualitative comparison on our method and the *P-SeqFuse* baseline. As illustrated in the figures, our methods could correctly understand the referring expression and localize object mask accordingly. By contrast, the compared method may fail to follow the text guidance, leading to less accurate segmentation results.

### Additional Examples of Expert Routing on VQAv2

Our MoPE is designed to scale up the expressiveness of vanilla prompts, and expert specialization is a critical condition to achieve superior results as well as interpretability. In the main body of the paper, we have provided visualization results of expert routing on the SNLI-VE dataset. We found the expert specialization are more observable on large dataset with a high heterogeneity. Hence, to further demonstrate expert specialization, we train our MoPE-based method on an even larger dataset, VQAv2 (Goyal et al. 2017). This dataset contains 265,016 images and paired questions, covering a wide array of visual and textual concepts. We train our model on this dataset and visualize the routing results in Figures 12, 13, 14, and 15. We observe clear expert specialization in these examples, where different experts capture different concepts.

Prompt: "boy sitting on the bench closest to us"



Prompt: "center man with black hair back to us"



Prompt: "second from the right"



Prompt: "red shirt"



Prompt: "man"



Ground truth

P-SequentialFuse

Ours

Figure 10: Visualization on Referring Expression Segmentation - 1

Prompt: "lamb right"



Prompt: "sheep back left"



Prompt: "left sandwich"



Prompt: "left man"



Prompt: "girl chef on right of group"



Ground truth

P-SequentialFuse

Ours

Figure 11: Visualization on Referring Expression Segmentation - 2



